Pattern formation in oscillatory complex networks consisting of excitable nodes

Xuhong Liao,[1] Qinzhi Xia,[1] Yu Qian,[2] Lisheng Zhang,[1] Gang Hu,[1,*] and Yuanyuan Mi[1,†]
[1] *Department of Physics, Beijing Normal University, Beijing 100875, China,*
[2]*Nonlinear Research Institute, Baoji University of Arts and Sciences, Baoji 721007, China*
(Received 18 August 2010; revised manuscript received 4 November 2010; published 4 May 2011)

Oscillatory dynamics of complex networks has recently attracted great attention. In this paper we study pattern formation in oscillatory complex networks consisting of excitable nodes. We find that there exist a few center nodes and small skeletons for most oscillations. Complicated and seemingly random oscillatory patterns can be viewed as well-organized target waves propagating from center nodes along the shortest paths, and the shortest loops passing through both the center nodes and their driver nodes play the role of oscillation sources. Analyzing simple skeletons we are able to understand and predict various essential properties of the oscillations and effectively modulate the oscillations. These methods and results will give insights into pattern formation in complex networks and provide suggestive ideas for studying and controlling oscillations in neural networks.

DOI: 10.1103/PhysRevE.83.056204 PACS number(s): 89.75.Kd, 05.65.+b, 89.75.Fb

I. INTRODUCTION

Many social and natural systems have been well described by complex networks [1–4]. Complex networks with excitable local dynamics have attracted particularly great attention for their wide applications, such as epidemic spreads [5,6], chemical reactions [7], biological tissues [8,9], among which neural networks are typical examples [8–11]. Complexity of network structures and excitability of local dynamics are two major characteristics of neural networks [12,13]. Oscillations in these networks determine rich and important physiological functions [14,15], such as visual perception [16], olfaction [17], cognitive processes [18], and sleep and arousal [19]. Therefore, oscillations in neural networks and other excitable networks have been studied extensively.

Problems of pattern formation in these excitable systems call for further investigation, because early works on pattern formation focused on patterns in regular media [20–22]. It is natural to ask what pattern formation looks like in complex networks, and whether there are some common rules in different types of networks. Very recently, Turing patterns in large random networks have been discussed by Hiroya Nakao *et al*. [23]. In the present paper we study another type of pattern, self-sustained oscillatory patterns in complex networks consisting of excitable nodes, which are important in physics, chemistry, and biology. Since each excitable node cannot oscillate individually [24], there must exist some delicate structures supporting the self-sustained oscillations [10,11,25,26]. So far, some concepts, such as recurrent excitation [10,25,27,28] and central pattern generators [29–31], have been proposed to describe these structures. However, if networks consist of large numbers of nodes and random interactions, it is difficult to detect these structures [11,26]. In previous papers [32,33], we proposed a method of dominant phase advanced driving (DPAD) to study the phase relationship between different nodes based on oscillatory data. Oscillation sources for self-sustained oscillations are identified successfully. However, the topological effects on the dynamics are not fully understood.

The interplay between the topological connectivity and the network dynamics has become one of the central topics under investigation [34–36]. The present paper is to explore the mechanism of pattern formation in oscillatory excitable networks and unveil the topological dependence of the oscillations. This paper is organized as follows. Section II introduces the excitable networks of the Bär model. Simulation results are provided in Sec. III, where center nodes and target waves are identified. In Sec. IV, the skeletons of different oscillations are displayed to unveil the topological effects on network dynamics. In Sec. V results in previous sections are extended to networks with different sizes and degrees. Section VI gives extensions to excitable scale-free networks. Networks with the Fitzhugh-Nagumo model as local dynamics are also discussed. The conclusions are given in Sec. VII.

II. MODEL OF NETWORKS

We consider complex networks consisting of N excitable nodes. The network dynamics is described as follows:

$$\begin{aligned} \frac{du_i}{dt} &= -\frac{1}{\varepsilon}u_i(u_i-1)\left(u_i-\frac{v_i+b}{a}\right)+D_u w_i, \\ \frac{dv_i}{dt} &= f(u_i)-v_i, \quad i=1,2,\ldots,N \\ w_i &= \frac{\sum_{j=1}^{N} M_{ij}u_j}{\sum_{j=1}^{N} M_{ij}u_j+K}-u_i, \\ f(u_i) &= \begin{cases} 0, & u_i < \frac{1}{3}, \\ 1-6.75u_i(u_i-1)^2, & \frac{1}{3} \leqslant u_i \leqslant 1, \\ 1, & u_i > 1. \end{cases} \end{aligned} \tag{1}$$

The Bär model is adopted as local dynamics [37], where parameters $\{a,b,\varepsilon\}$ are properly set so that each node possesses excitable local dynamics. The adjacency matrix M_{ij} is defined by $M_{ij}=1$ if node i is connected with node j and $M_{ij}=0$ otherwise. Coupling w_i represents the total interaction on a given node i from all its neighbor nodes. This form of coupling is used to ensure that any excited node can excite

*ganghu@bnu.edu.cn
†miyuanyuan0102@163.com

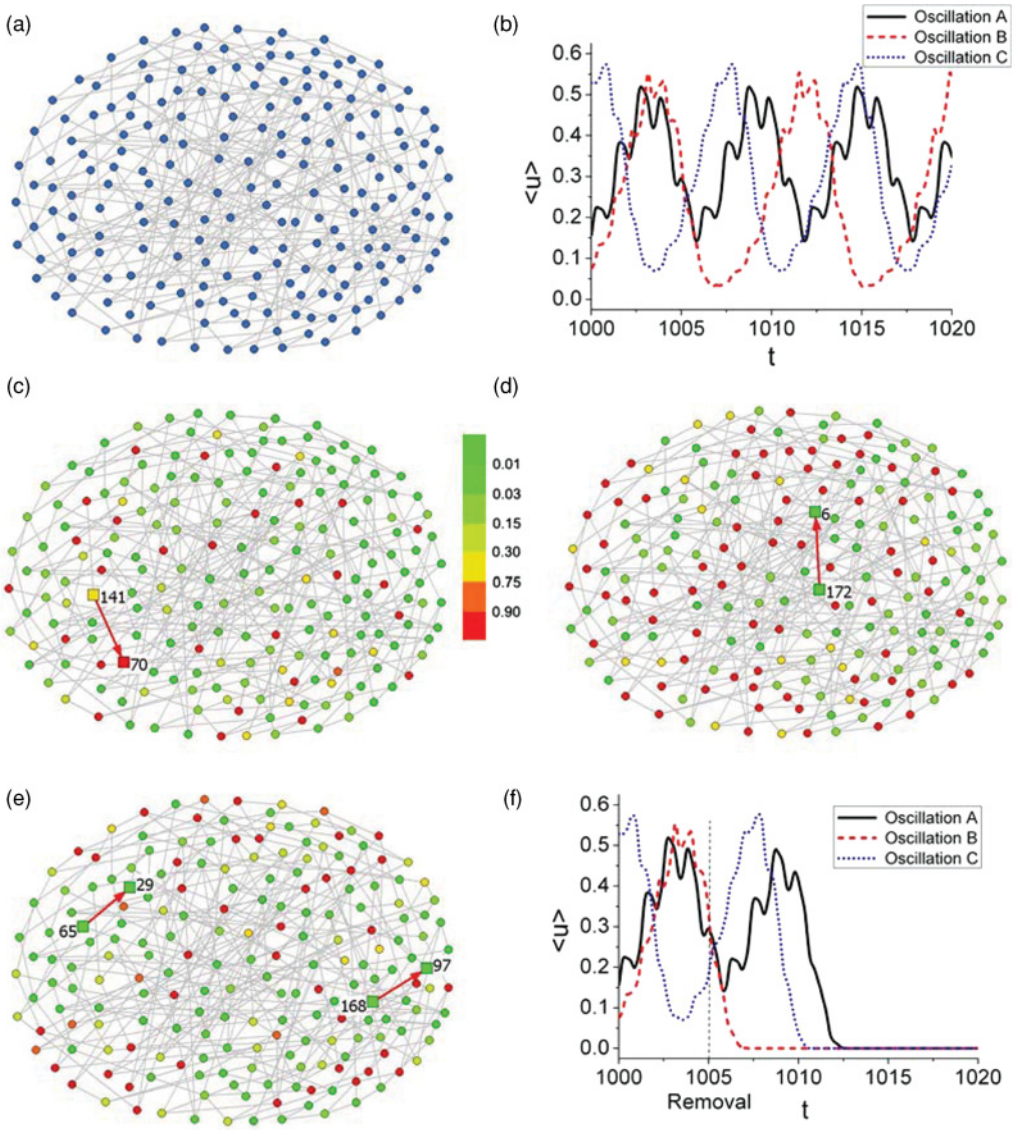

FIG. 1. (Color online) (a) Homogeneous random network studied. $N = 200$, $k = 3$. The network dynamics is described by Eq. (1) with parameters $a = 0.84$, $b = 0.07$, $\varepsilon = 0.04$, $D_u = 0.4$, $K = 0.8$. All these parameters are used in Figs. 1–5. (b) Periodic time evolution of $< u(t) >= 1/N \sum_{i=1}^{N} u_i(t)$ for three different random initial conditions. These three oscillations are denoted as oscillations A, B, and C, respectively. (c) Snapshot of oscillation A at a certain time. The phase distribution among different nodes seems random. In the following figures, all snapshots are displayed with local variable u plotted without further remarks, and the arrowed links in all figures represent the dynamical driving relationship. (d) and (e) Snapshots of oscillations B and C, respectively. (f) Suppression of oscillations A, B, and C by removing square nodes 70, 6, and (29, 65) at $t = 1005$, respectively. The time of node removal is denoted by the vertical dashed line.

its rest neighbor nodes with proper values of D_u and K. Other forms of coupling, which have similar effects, are also feasible, such as diffusive coupling. This type of interaction has been widely used in neural models [9,10,25] and other excitable networks [5,38,39]. During the simulations, different types of networks are generated, and the connections between different nodes are bidirectional and symmetric. For simplicity, we study, first, homogeneous random networks with an identical degree k; i.e., each node interacts with an equal number of k nodes randomly chosen. Meanwhile, we assume that all nodes have identical parameters so that any heterogeneity in network patterns is not due to the topological inhomogeneity but results from the self-organization in nonlinear dynamics. In the present paper we focus on the self-sustained periodic oscillations.

III. CENTER NODES AND TARGET WAVES

The homogeneous random network studied is displayed in Fig. 1(a). With the parameters given, the system has a large probability (about 95%) to approach periodic oscillations from random initial conditions. Moreover, different initial conditions approach different oscillations in most cases. For instance, we observed 961 different oscillations within

1000 tests, and the other samples reached the rest state. The evolution of average signals $< u(t) >= 1/N \sum_{i=1}^{N} u_i(t)$ for three different oscillations A, B, and C is displayed in Fig. 1(b). These three oscillations have different periods ($T_A = 5.99$, $T_B = 8.37$, $T_C = 7.00$ with $T_{A,B,C}$ being periods of oscillations $A, B,$ and C, respectively). In Figs. 1(c)–1(e) spatial snapshots of oscillations A, B, and C are plotted, respectively. All these patterns have seemingly random phase distributions, in which the structures supporting the oscillations are deeply hidden.

We start our analysis from local dynamics of excitable networks. Because each node is an excitable system [24,37], the individual node will stay at the rest state forever without perturbation. Since there is no external pacemaker in the network, there must be some loops to support the self-sustained oscillations, where nodes can be repeatedly excited in sequence. Therefore, it is natural to conclude that the topological loop structure of complex networks is crucial for the network oscillations [25,26,32,33]. However, in complex networks there are extremely large numbers of loop sets [for the network in Fig. 1(a) with $N = 200$ nodes and $M = 300$ interactions, there are $2^{101} - 1$ loop sets [40]]. A crucial question is which loop set plays the essential role for a given oscillation. Because nodes in the network are excited in sequence, all waves propagate forward along the shortest paths [9,25,26]. The loops dominating the oscillations must obey this "shortest path" rule, which means the source loops should be as short as possible. Furthermore, due to the existence of the refractory period, these loops must also be sufficiently large to maintain the recurrent excitation. Here the problem remained is how to reveal these shortest loops.

We study the above loop problem by making perturbation to each oscillation and observe the system's response. A few nodes randomly chosen are removed from the network at each test. (Here removing a node means discarding all interactions of this node.) In most cases the oscillation is robust. However, we find to our surprise that the oscillation is crucially sensitive to some specific nodes. These specific nodes for a given oscillation are defined as key nodes, among which a minimum number of nodes can be removed to suppress the oscillation. In Figs. 1(c)–1(e) different key nodes for oscillations A, B, and C are displayed with large squares, respectively. Both oscillations A and B can be suppressed by just removing one key node, as shown in Fig. 1(f). However, we can never suppress oscillation C by removing any single node. There are two pairs of key nodes displayed in Fig. 1(e). In order to terminate oscillation C [see also Fig. 1(f)], we have to remove two key nodes simultaneously, one from the pair (29,65) and the other from the pair (97,168). The diverse behavior displayed in Figs. 1(c)–1(e) indicates that even though the parameter distributions and the node degrees are homogeneous in the network, the dynamical patterns have delicate and heterogeneous self-organized structures where different nodes play significantly different roles in the oscillations.

We find further that all key nodes for these oscillations appear in directly interacted pairs. In each pair one node drives the other, i.e., $141 \rightarrow 70$, $172 \rightarrow 6$, and $65 \rightarrow 29$, $168 \rightarrow 97$. (The bidirectional link between nodes i and j is denoted by an arrowed link $i \rightarrow j$, if the interaction from node i is favorable for exciting node j from the rest state.) Considering the crucial influence of key nodes on the oscillations, we suggest that the function of the driven nodes is to excite the whole network, while the function of the driving ones is to keep their partners oscillating. Thus these driven nodes (70 for A, 6 for B, 29 and 97 for C) are regarded as center nodes for the oscillations, while the driving ones are regarded as the drivers of the center nodes. An oscillation with n centers is called an n-center oscillation. Both oscillations A and B are one-center oscillations, while oscillation C is a two-center oscillation.

TABLE I. Number of center nodes for different oscillations in Homogeneous Random Networks (HRNs). Parameters (a, b, ε, D_u) are set the same as in Fig. 1, except constant K ($K = 0.8$ for HRNs with $N = 100$, 200 and $K = 1.8$ for other networks). One thousand different networks are investigated with random initial conditions for the statistics in each column.

N	100	200	200	1000	2500	$SF200$[a]
k	3	3	5	7	8	$< k >= 4$
Periodic oscillations	785	955	675	549	328	172
One-center	290	98	191	457	298	156
Two-center	244	172	170	85	30	15
Three-center	144	199	97	7	0	1
Four-center	52	189	73	0	0	0
Others[b]	55	297	144	0	0	0

[a]Scale-free networks with average degree$< \kappa >= 4$.
[b]Periodic oscillations with more than four centers.

The existence of key nodes and center nodes is general for periodic oscillations in excitable complex networks. We investigated Eq. (1) with random initial conditions for different networks and sampled stable periodic oscillations. The transient time for each oscillation depends on the network size N. When the network size increases, the transient will be prolonged. Moreover, the transient time is also effected by the type of the pattern. Generally speaking, the more center nodes the pattern has, the longer the transient needs to be. When the oscillation reached stability, center nodes were identified. Numbers of center nodes for most oscillations are listed in Table I. For other oscillations remained, we did not make a further search, because identifying more than four center nodes is very computationally consuming. Anyway, we find that most oscillations have self-organized structures with an extremely small number of center nodes. Thus the features of oscillations $A, B,$ and C can be identified as the typical behavior of self-sustained oscillations in excitable complex networks.

Because of the significant effects of center nodes on oscillations, we expected that the source loops of the oscillations must be around the center nodes. Further study confirmed the expectation. We identified that there are just some well-organized loop structures around the center nodes to maintain the self-sustained oscillations. Two principles are proposed for pattern formation in a given network oscillation.

(1) Waves propagate forward from center nodes to the whole network along the shortest paths.

(2) The shortest loops, which pass through both the center nodes and their driver nodes, play the role of oscillation sources and dominate the oscillation behavior.

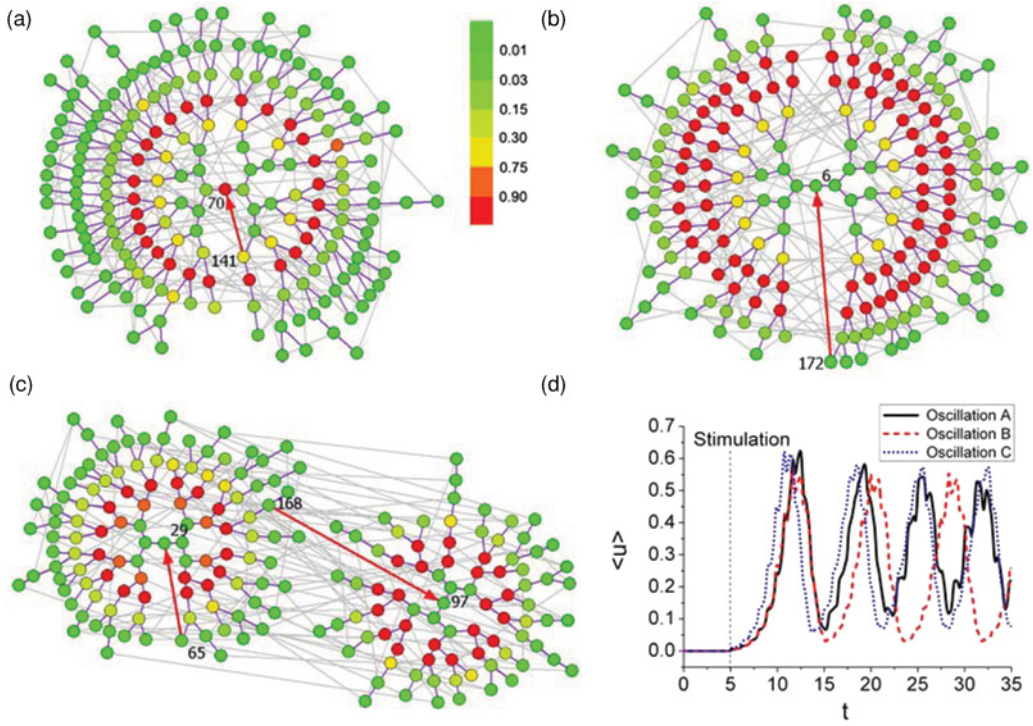

FIG. 2. (Color online) (a) Snapshot is the same as in Fig. 1(c) for oscillation A, with each node placed around center node 70 according to the distance from the center. The purple (dark) lines show the shortest paths from center node 70 to the other nodes, while the gray (light) lines mean all the other interactions between different nodes. Perfect target waves are observed propagating from center node 70. The bold arrow denotes the driving from node 141 to center node 70. (b) Snapshot is the same as in Fig. 1(d) for oscillation B. The target center is node 6, while its driver is node 172. (c) Snapshot is the same as in Fig. 1(e) for oscillation C, with nodes placed around two centers 29 and 97. Two-center target pattern is identified. (d) Creation of oscillations A, B, and C by initially stimulating a few center nodes [node 70 for A, node 6 for B, nodes (29, 65) for C]. Average signals $< u(t) >$ for different oscillations are displayed. Stimulations are performed at $t = 5$ denoted by the vertical dashed line.

With these two principles we can clearly reveal oscillation sources, illustrate wave propagation paths, and unveil the topological effects on the oscillations.

Based on the first principle, we can demonstrate the oscillatory pattern for each oscillation according to a simple placing rule as follows. At first, place each center node at a certain position. Second, if there is only one center node, locate all the other nodes around this center according to the distances (shortest paths) from it. However, if there are two synchronous centers, two clusters of nodes will exist, each around a center. The other nodes should select the cluster with the "nearest" center node before the rearrangement. During the cluster selection if a node has the same distance from both centers, it can be included to either cluster. This simple placing rule transforms all random patterns into well-behaved target waves. A similar operation can be applied to oscillations with more centers. Snapshots of oscillation A, B, and C in a new order are displayed in Figs. 2(a)–2(c), respectively, which are exactly the same as those in Figs. 1(c)–1(e). In these figures surprisingly well-ordered target waves are observed, one-center target waves for oscillations A and B, and two-center target waves for oscillation C, which are in sharp contrast with the random phase distributions in Figs. 1(c)–1(e). All nodes are driven by waves emitting from center nodes, and the importance of the center nodes is demonstrated clearly. The recurrent excitation of the center nodes via the driving key nodes is the reason why the center nodes can keep oscillating to excite the whole network. It is instructive to observe these self-sustained target waves in oscillatory random networks and demonstrate how these waves self-organize. On the basis of these target patterns, different oscillation sensitivities observed in Fig. 1 can be understood. First, due to the one-center target structure of Figs. 2(a) and 2(b), we can definitely terminate the oscillation by removing a center node (70 for A, 6 for B), since the center node is the only wave source. The oscillation can also be suppressed by removing the driving node (141 for A, 172 for B) because the driving node is the only driver of the center node, without which the center can no longer oscillate sustainedly. Second, since oscillation C has a structure of two-center target waves, removing any single key node cannot destroy the oscillation sources completely. Both target centers (or their drivers) should be removed simultaneously to suppress this two-center oscillation. Similarly, in order to terminate an oscillation with n centers, n centers (drivers) should be removed simultaneously.

In Fig. 1(f) effective suppression of given oscillations is displayed. However, how to create a given oscillation with high efficiency is still not clear. Excitable networks, such as that in Fig. 1(a), have a huge number of attractors, each of which has a small basin of attraction. If we try to reach a given oscillation by random initial conditions we may need thousands or even millions of tests that are computationally

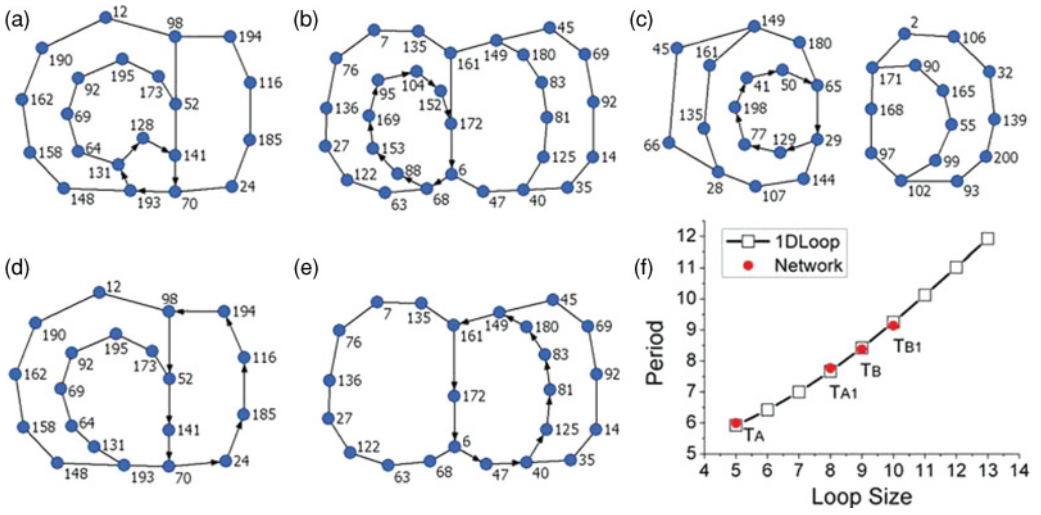

FIG. 3. (Color online) (a)–(c) Skeletons of oscillations A, B, and C, respectively. (a) Skeleton of oscillation A consisting of all loops passing through key nodes (70, 141) with length $L \leqslant 10$. (b) Skeleton of oscillation B consisting of all loops passing through key nodes (6,172) with length $L \leqslant 11$. (c) Skeleton of oscillation C consisting of all loops passing through the key node pair (29,65) or the other pair (97,168) with $L \leqslant 10$. (d) Skeleton of oscillation A_1 with node 128 removed from oscillation A. (e) Skeleton of oscillation B_1 with node 88 removed from oscillation B. (f) Oscillation periods versus the driving shortest loops identified. The white squares in the solid curve represent numerical results for one-dimensional loops, which have the same parameters as those in Fig. 1. T_A, T_B, T_{A_1}, T_{B_1} (red (dark) circles) denote periods of oscillations A and B and their modulated oscillations A_1 and B_1. All circles are located around the squares.

consuming and practically unreasonable. However, when the center nodes and their drivers are identified, we can recover a given oscillation with high efficiency by manipulating only a very few nodes. To create oscillation A (B) from the all-rest state we only need to initially stimulate single center node 70 (6) while the interaction from the center node to its driving key node 141 (172) is blocked during the initial excitation period of the center node. We find that the excitation activities propagate away from the center node and then come back via the driving key node to reexcite the center node. Then the system evolves autonomously to target pattern A (B) via the self-organized excitation propagation in the network. Generally speaking, we can recover any given n-center target pattern by initially stimulating n centers with the interactions from these centers to their drivers blocked during the initial excitation periods of center nodes. In the following paper, this excitation procedure is briefly called n-center node excitation, without additional remarks on the interaction modulations. In Fig. 2(d) we present the evolution generated by one-node-excitation with the solid (dashed) curve, which recovers oscillation A (B) asymptotically. In order to recover oscillation C, both center nodes 29 and 97 should be excited simultaneously. The creation of oscillation C is shown by the dotted curve in Fig. 2(d).

IV. SKELETONS AND OSCILLATION CONTROL

Based on principle 2, we can construct a skeleton and reveal the oscillation source for each oscillation by analyzing the network topology. The skeleton of a given oscillation means a subnetwork consisting of some short topological loops passing through both the center nodes and their drivers. Topological effects on a network oscillation can be well unveiled based on the skeleton. In Figs. 3(a)–3(c) skeletons of oscillations A, B, and C are displayed, respectively. In Fig. 3(a) we display all topological loops with length $L \leqslant 10$, passing through the pair of key nodes (70, 141). In Fig. 3(b) the skeleton of oscillation B is plotted, consisting of loops with length $L \leqslant 11$ passing through the key node pair (6,172). An interesting difference between Figs. 3(a) and 3(b) is that the shortest loop in Fig. 3(a) [$L_{\min}(A) = 5$] is much smaller than that in Fig. 3(b) [$L_{\min}(B) = 9$]. In Fig. 3(c) we show the skeleton of oscillation C consisting of loops with length $L \leqslant 10$, passing through the pair of nodes (29, 65) or (97, 168). The skeleton supporting oscillation C consists of two clusters with $L_{\min}(C) = 7$. Furthermore, for each oscillation under investigation the shortest loops displayed in the skeleton always have a successive driving relationship. In Figs. 3(a)– 3(c), these successive driving shortest loops are indicated by arrows. These driving loops, supporting self-sustained oscillations of the center nodes, are regarded as the oscillation generators. The phenomenon in Fig. 1(b) that oscillations A, B, and C have different periods ($T_A = 5.99$, $T_B = 8.37$, $T_C = 7.00$) can be understood from these oscillation generators. It has been known that a pulse can circulate along a one-dimensional (1D) loop consisting of excitable nodes. The period of the oscillation increases as the loop's length increases [41]. Since the shortest loop in each skeleton dominates the oscillation, we have the conclusion $T_B > T_C > T_A$ for $L_{\min}(B) > L_{\min}(C) > L_{\min}(A)$. That is the reason why different oscillations may have different periods.

The structures of skeletons in Figs. 3(a)–3(c) are greatly simplified in contrast with the original complex network in Fig. 1(a). They contain a much fewer number of nodes and reduce the original high-dimensional complex structure to various sets of 1D loops. It is important to find these small skeletons, which indicate many essential features of the network oscillations. We can efficiently modulate the oscillations

just by analyzing these simple skeletons. In the following discussion the oscillation period is taken as a measurable quantity to demonstrate the oscillation modulations.

First, we modify oscillation A by removing node 128. This operation changes oscillation A to oscillation A_1. Based on Fig. 3(a) we can predict the network evolution after the modulation. First, although the shortest five-node loop is destroyed, there are still some other loops containing center 70 and its driver 141. The oscillation will be maintained. Second, the new shortest loop among the remaining loops will emerge as a dynamical loop, which guarantees the recurrent excitation of center 70 and maintains the network oscillation. Because the length of the new shortest loop ($70 \rightarrow 24 \rightarrow 185 \rightarrow 116 \rightarrow 194 \rightarrow 98 \rightarrow 52 \rightarrow 141 \rightarrow 70$) is 8, we expect that the modified oscillation A_1 must have a larger period. Our predictions are confirmed. The skeleton of oscillation A_1 is shown in Fig. 3(d), where the right loop (marked by the arrowed loop) actually emerges as the oscillation generator. And the period of oscillation A_1 is indeed larger than that of oscillation A ($T_{A_1} = 7.77 > T_A = 5.99$). Similar operations are applied to oscillation B. Oscillation B_1 is obtained by removing single node 88 from oscillation B. Analyzing the skeleton in Fig. 3(b) we expect that this operation must prolong the original period T_B to T_{B_1} ($T_{B_1} > T_B$), for the new shortest loop has a length $L = 10$. In Fig. 3(e) the skeleton of oscillation B_1 is displayed as expected. Then we find $T_{B_1} = 9.14 > T_B = 8.37$. In Fig. 3(f) periods of 1D oscillatory loops with different sizes are displayed with white squares in the solid curve. Periods of network oscillations A, B, A_1, and B_1 are also displayed with red (dark) circles. Both sets of periods coincide well. It demonstrates that simplified skeletons indicate essential features of complicated patterns, and the shortest loops, which pass through both the center nodes and their drivers, indeed dominate the dynamics of the network oscillations.

The modulation diversity can be much richer for oscillations with more centers. Different modulations are applied to oscillation C. In the subsequent paragraphs, responses of oscillation C to the removal of different nodes, (1) node 97, (2) node 29, and (3) nodes 129 and 99, will be studied. We find that all simulations of the network oscillations fully coincide with predictions from the simple skeleton in Fig. 3(c).

(1) If center node 97 is removed, the network oscillation must change, i.e., from oscillation C to C_1. Analyzing the skeleton of oscillation C, the right subskeleton must be destroyed by removing its center 97, while the left subskeleton is remained intact to support oscillation C_1. Since only left target center 29 works, the original two-center target pattern must be transformed to a one-center target pattern, and the nodes in the original right cluster must move to the left cluster. The left cluster will grow from the boundary with nodes migrating from the destroyed cluster. We present the target pattern of oscillation C_1 in Fig. 4(a) by simulation and find a pattern the same as we predicted. In Fig. 4(b) we plot the skeleton of oscillation C_1, which is nothing but the left subskeleton in Fig. 3(c). (2) If center node 29 is removed from oscillation C, the left subskeleton in Fig. 3(c) is destroyed. The resulting oscillation is denoted by C_2. We expect that node 97 will work as the only center, and the shortest loop in right subskeleton will work as the oscillation generator. In Figs. 4(c) and 4(d) we observe that all predictions are fully confirmed. (3) If two nodes are removed simultaneously, node 129 from the left cluster and node 99 from the right one, oscillation C_3 is generated. We predict from Fig. 3(c) that the two-center target pattern should be maintained (since the functions of two centers are preserved), and the skeleton of C_3 can be deduced from Fig. 3(c) with the shortest loops in both clusters destroyed. Then we stimulate oscillation C_3 and plot a snapshot by arranging the nodes in order. Two-center target waves are verified in Fig. 4(e). The skeleton of oscillation C_3 is displayed in Fig. 4(f). Both Figs. 4(e) and 4(f) fully confirm the above predictions.

Meanwhile, the above operations have adjusted the oscillation periods. In case 1 since the oscillation generator of C_1 remains the same as that of oscillation C, the resulting period T_{C_1} should remain approximately the same as T_C. For oscillation C_2 in case 2, the new oscillation generator (the arrowed shortest loop) in Fig. 4(d) has length 8, and then period T_{C_2} should increase to about 7.66 by comparison with 1D loop data in Fig. 4(g). Since loop nodes 129 and 99 are removed in case 3, oscillation C_3 has the shortest source loops of length 9 [arrowed loops in the left cluster in Fig. 4(f)]. Thus period T_{C_3} should be close to 8.42 [see Fig. 4(g)], which is considerably larger than T_C. In Fig. 4(g) numerical results of the modulated networks are compared with those of 1D loops. Both sets of data agree well with each other. It is amazing that by removing node 97 we dramatically change the oscillation pattern while keeping the period almost unchanged. In contrast, by removing two nodes (129, 99) we keep the two-center target pattern while largely slowing down the oscillation. All these seemingly strange responses can be well explained with the skeleton in Fig. 3(c).

So far, we discussed oscillations A, B, and C in the given network Fig. 1(a) in detail. However, oscillation patterns in a complex network are much more abundant. The choice of key nodes and related source loops depends on initial conditions, because the basins of attraction of different attractors may be very complicated in nonlinear dynamic systems. For a homogeneous random network all nodes are topologically equivalent, and each node may play a role of a center node or the driver of the center node. The only condition is that the shortest loops passing through both the center node and its driver must be large enough to guarantee the recurrent excitation.

V. COMPLEX NETWORKS WITH DIFFERENT SIZES AND DEGREES

Till now we have focused on Eq. (1) with $N = 200$ and $k = 3$. All characteristics observed in this particular case can be extended to networks with different sizes and degrees. Here we study another example of Eq. (1) with $N = 400$ and $k = 4$. The network structure is displayed in Fig. 5(a). With a certain initial condition we observe an oscillation Φ with a snapshot shown in Fig. 5(b). This oscillatory pattern has seven key nodes, which are displayed with squares in Fig. 5(b). Four centers (4, 57, 176, 260) are identified. Removing four key nodes simultaneously from four different sets, i.e., one node from each set, we can suppress this oscillation. This process is displayed by the solid curve in Fig. 5(c). Different from

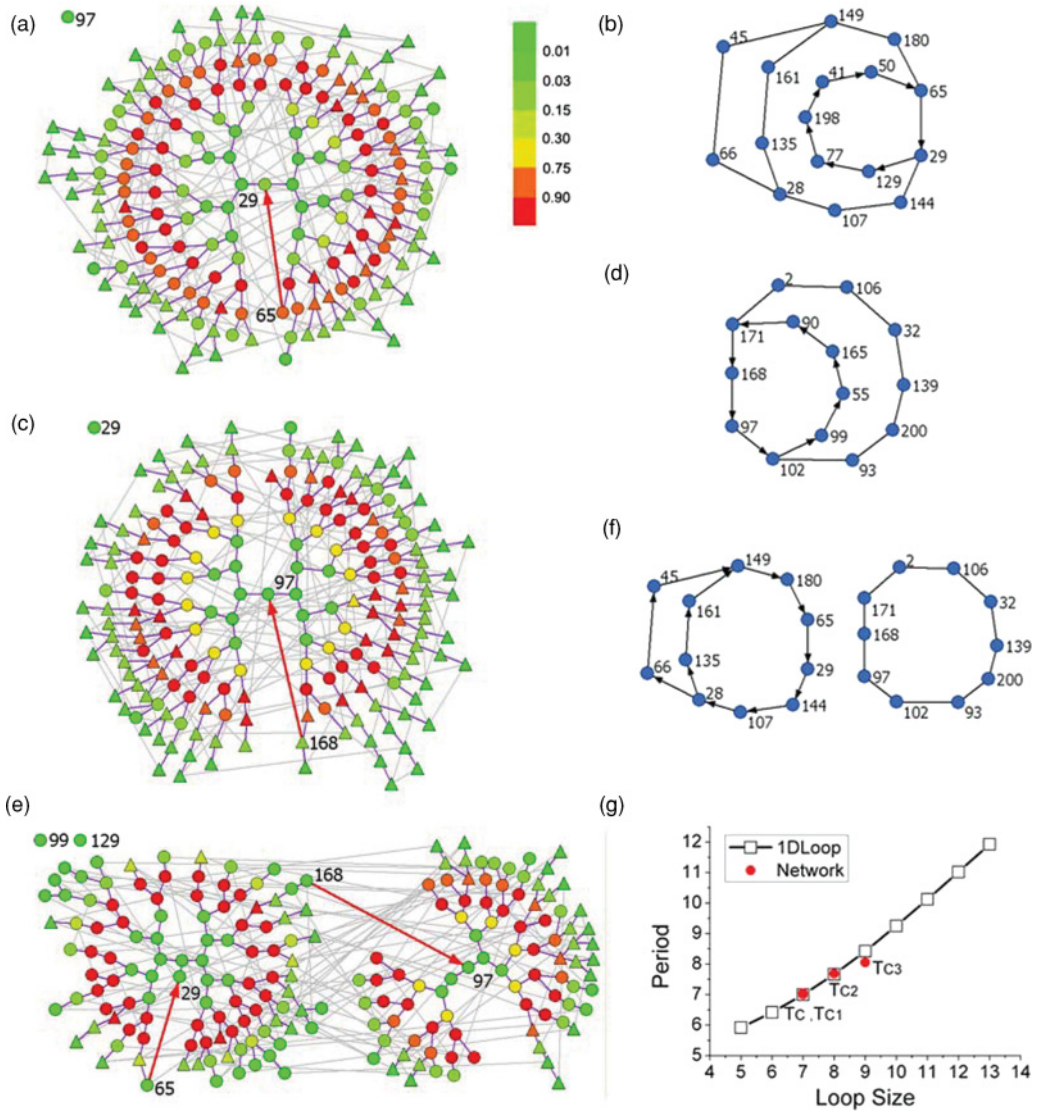

FIG. 4. (Color online) (a) Snapshot of oscillation C_1 with center node 97 removed from oscillation C [see Fig. 2(c)]. Triangles denote the nodes migrating between different clusters after the modulation. (b) Skeleton of oscillation C_1. (c) Snapshot of oscillation C_2 with center node 29 removed from oscillation C. (d) Skeleton of oscillation C_2. (e) Snapshot of oscillation C_3 with two nodes (129, 99) removed from oscillation C simultaneously. (f) Skeleton of oscillation C_3. (g) Periods T_C and T_{C_i}, $i = 1, 2, 3$ (red (dark) circles) versus the lengths of the shortest loops in the skeletons. All data of T_{C_i} can be approximately predicted by the results of 1D loops (white squares in the solid curve).

oscillations A, B, and C, in Fig. 5(b) only three sets of key nodes appear in pairs [such as (57, 339), (176, 13), (260, 382)], while key node 4 appears without any partner. The reason is the following. Since each node has a degree $k = 4$, a center node may have a single dynamical driver (such as $339 \rightarrow 57$, $13 \rightarrow 176$, $382 \rightarrow 260$) or multiple drivers [such as node 4 in Fig. 5(d), having two drivers 244 and 360]. If a center node has only one driver, the driver node also becomes a key node for controlling the center node. However, when the center node has multiple drivers, removing one of these drivers cannot terminate the function of the center. Thus this center node does not have a partner node for the oscillation suppression. Similar to Fig. 2(d) we can generate an oscillatory pattern in Fig. 5(d) from the all-rest state by initially stimulating the four centers (4, 57, 176, 260) with interactions from these centers to their drivers blocked during the initial excitation periods of the center nodes. Time evolution of this oscillation generation is shown in Fig. 5(c) with the dotted curve.

In Fig. 5(d) we show exactly the same snapshot as that in Fig. 5(b) with all nodes rearranged in four clusters according to their distances from different centers, i.e., each node chooses the cluster with the "nearest" center node, and then it is placed in the selected cluster according to the distance from the center. Different sizes of four clusters result from the asynchronous excitation of different centers. If an oscillatory pattern has multiple centers, each center emits excitation waves and controls a cluster of nodes. A node will belong to the ith cluster if the excitation wave from the ith center reaches this node first in comparison with the other centers. Therefore, if all centers have synchronous excitation any given node is controlled by the nearest center, as we did in Fig. 2(c). If multiple centers are not synchronous, i.e., they are excited

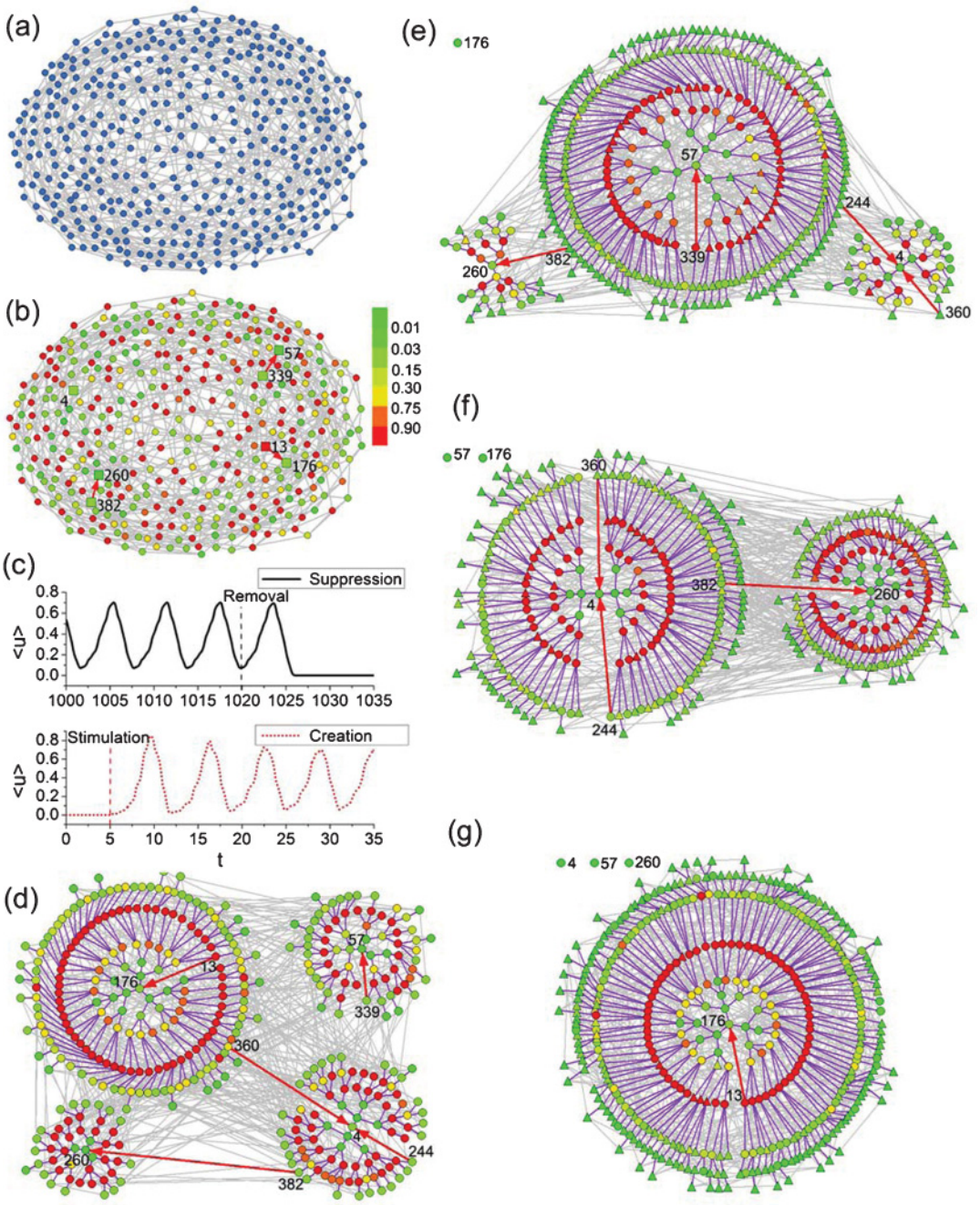

FIG. 5. (Color online) (a) Homogeneous random network with $N = 400$, $k = 4$. The other parameters are the same as those in Fig. 1. (b) Snapshot of oscillation Φ generated randomly. Four sets of key nodes are displayed with squares. (c) Suppression and creation of oscillation Φ. Removing simultaneously four center nodes (4, 57, 176, 260) can suppress the oscillation as shown by the solid curve. Oscillation Φ can also be generated by initially stimulating four center nodes (4, 57, 176, 260), as shown by the dotted curve. Different operation times are denoted by the vertical dashed lines. (d) Snapshot is the same as (b) for oscillation Φ, with nodes are rearranged in order. (e)–(g) Snapshots of oscillations after different modulations to oscillation Φ. Triangles mean the nodes migrating between different clusters after the modulations. (e) Snapshot of three-center oscillation with center 176 removed from oscillation Φ. (f) Snapshot of two-center oscillation with two centers (57, 176) removed from oscillation Φ. (g) Snapshot of one-center oscillation with three centers (4, 57, 260) removed from oscillation Φ.

at different times, the measurement of the distance should be modified by counting the excitation time differences of various centers. In the case of oscillation Φ, four centers are excited at slightly different times. Specifically, in each round node 176 is excited first, nodes 57 and 4 have a single-step delay (one-step here means T/n, with T being the oscillation period and n being the number of nodes in a single wavelength), while node 260 has a two-step delay. Then the "nearest" center means the center node with the shortest distance among (d_1, $d_2 + 1$, $d_3 + 1$, $d_4 + 2$), with (d_1, d_2, d_3, d_4) being the actual topological distances from centers (176,57,4,260) to the given node. This method of distance measurement is applied to

all the patterns where more than one center exist. With this arrangement we find that the seemly random phase distribution in Fig. 5(b) is actually a well-behaved four-center target wave pattern. All the modulations to oscillation C shown in Fig. 4 can be applied to oscillation Φ in Fig. 5(b). For instance, by removing center 176 we can transform the original four-center target waves to three-center waves with centers 4, 57, and 260. All nodes migrating between different clusters after the modulations are also displayed by triangles in Fig. 5(e). In Figs. 5(f) and 5(g) we removed two center nodes (57, 176) and three center nodes (4,57,260), respectively. Two-center and one-center target patterns are found, where all the remaining centers emit target waves. All these modulation results show the generality of the two principles.

VI. EXTENSIONS

In the previous discussions we considered only homogeneous random networks where all nodes have the same degree. Both principles 1 and 2 can be extended to Erdös-Rényi (ER) networks and scale-free (SF) networks, which are inhomogeneous in topological structures. Results in these networks are similar. It has been known that functional networks of the human brain exhibit scale-free properties [8,42]. In Fig. 6(a) we present an example of a SF network with $N = 200$, $< k >= 4$. The size of each node i is proportional to the nature logarithm of its degree k_i. For this network we perform 1000 tests from different random initial conditions and find 142 self-sustained periodic oscillations. Among these oscillatory patterns we identify 128 oscillations with a single center, 13 oscillations with two centers, and one oscillation with three centers. The statistics for different networks is also listed in Table I. These results confirm that the existence of a small number of center nodes is also popular in inhomogeneous networks. In Figs. 6(b) and 6(c) we present two snapshots of different oscillations (one-center oscillation SF-A and two-center oscillation SF-B) from different initial conditions. The phase distributions seem complicated and random. However, some key nodes and center nodes for the oscillations are also identified (one pair of key nodes for oscillation SF-A

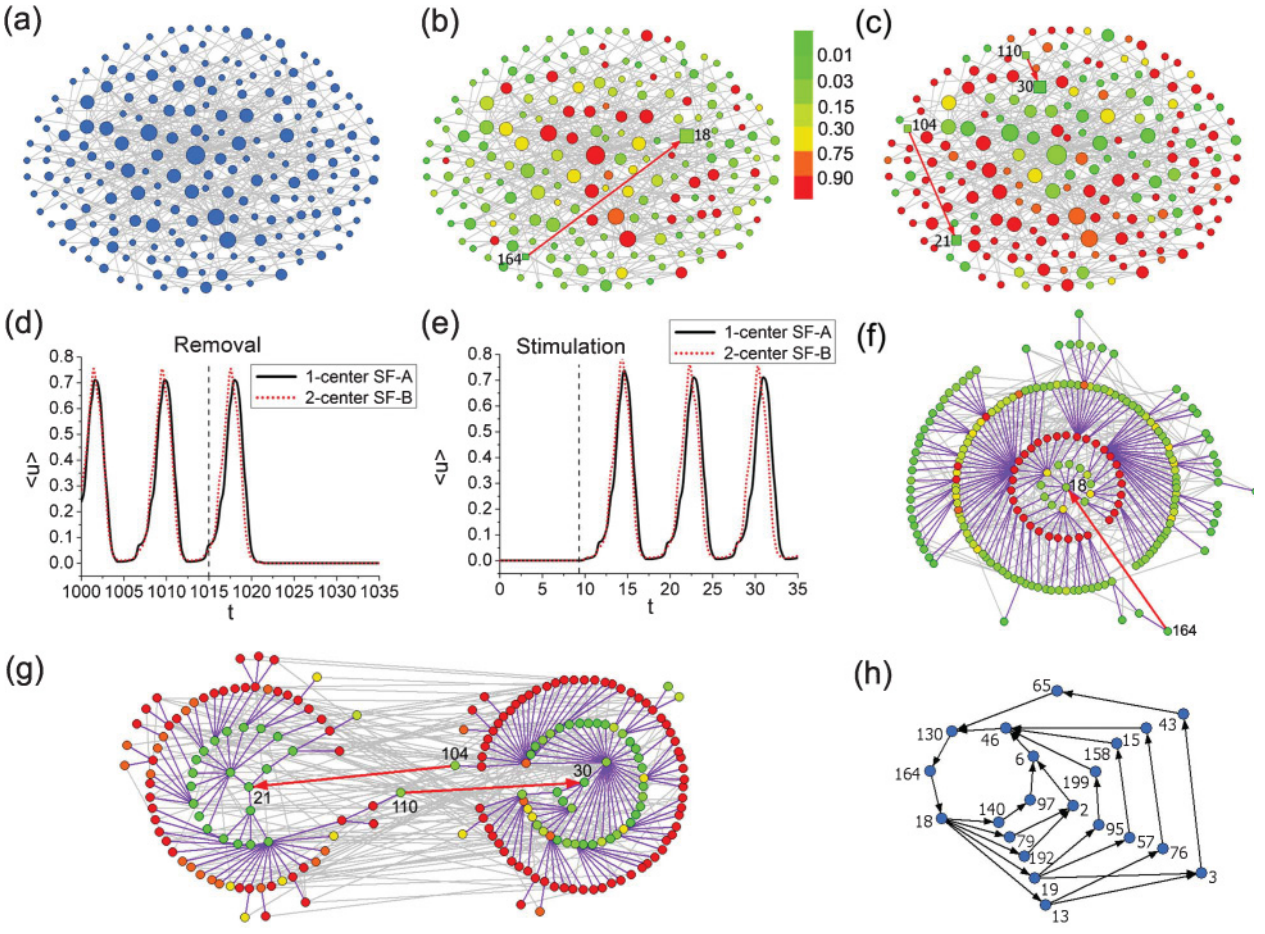

FIG. 6. (Color online) (a) SF network with $N = 200$, $< k >= 4$. The degree distribution obeys a power-law distribution with an exponent $\gamma = -3$. The size of each node i is proportional to $\ln(k_i)$. Parameters are set as follows: $a = 0.84$, $b = 0.07$, $\varepsilon = 0.04$, $D_u = 1.0$, $K = 1.8$. (b) Snapshot of oscillation SF-A with a single pair of key nodes denoted by squares. (c) Snapshot of oscillation SF-B with two pairs of key nodes identified. (d) Suppression of oscillations SF-A and SF-B by removing their center nodes [18 for SF-A and nodes (21, 30) for SF-B]. (e) Creation of oscillations SF-A and SF-B by initially stimulating the center nodes. (f) Snapshot is the same as (b) for oscillation SF-A, with nodes placed in order. One-center target waves are displayed. (g) Snapshot is the same as (c) for oscillation SF-B with nodes placed in order. Because two center nodes 21 and 30 are almost synchronous, nodes are arranged in the same way as in Fig. 2(c). Two-center target waves are observed. (h) Skeleton of oscillation SF-A, with all the shortest loops with length $L = 7$ displayed.

and two pairs for oscillation SF-B). The given oscillations can be suppressed [Fig. 6(d)] and created [Fig. 6(e)] by simply modulating the center nodes. In Figs. 6(f) and 6(g) we plot exactly the same snapshots as those in Figs. 6(b) and 6(c), respectively. With the placing rule, the random phase distributions of oscillations SF-A and SF-B can be rearranged to well-behaved one-center target waves [Fig. 6(f)] and two-center target waves [Fig. 6(g)], respectively. The skeleton of oscillation SF-A is shown in Fig. 6(h), based on which we can make oscillation modulations as we did in Fig. 4.

The only difference is that due to the high heterogeneity, there are many short loops passing through the pair of key nodes. In the skeleton shown in Fig. 6(h), only the shortest loops with $L = 7$ are demonstrated. Destroying any of the shortest loop will not significantly change the period of the oscillation, for the remaining shortest loops still have a length $L = 7$.

So far our investigation has been performed in networks with the Bär model as local dynamics. Actually, the principles can be also applied to other excitable systems. Here we study the Fitzhugh-Nagumo (FHN) model [24], which has been used for describing the dynamics of neural cells. Complex networks of FHN nodes with diffusive couplings are described as follows:

$$\frac{du_i}{dt} = \frac{1}{\varepsilon}\left(u_i - \frac{u_i^3}{3} - v_i\right) + D_u \sum_{j=1}^{N} M_{ij}(u_j - u_i)\,,$$

$$\frac{dv_i}{dt} = \varepsilon(u_i + \beta - \gamma v_i), \qquad i = 1,2,...,N. \quad (2)$$

In Fig. 7 we show a homogeneous random network under investigation with $N = 200$, $k = 3$. In Figs. 7(b)–7(h) we do the same as in Figs. 6(b)–6(h), respectively, with model Eq. (2) and network Fig. 7(a) considered. Apart from the skeleton [Fig. 7(h)] of the one-center oscillation, the skeleton of the two-center oscillation is also demonstrated in Fig. 7(i). Two

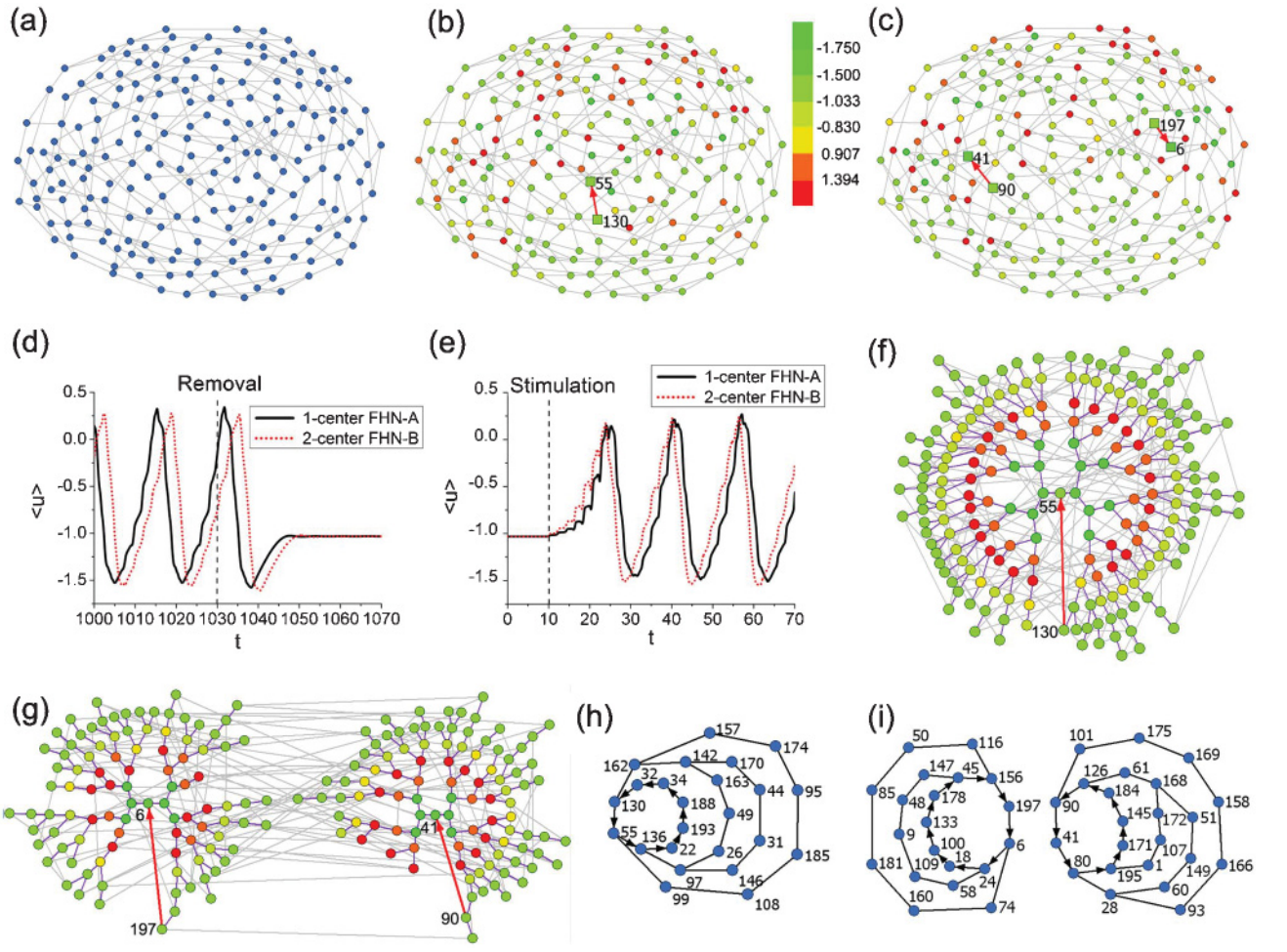

FIG. 7. (Color online) (a) Homogeneous random network considered with $N = 200$, $k = 3$. Network dynamics is described by Eq. (2). Parameters are set as follows: $\gamma = 0.5$, $\beta = 0.7$, $\varepsilon = 0.2$, and $D_u = 0.1$. (b) Snapshot of oscillation FHN-A with a single pair of key nodes. (c) Snapshot of oscillation FHN-B with two pairs of key nodes. (d) Suppression of oscillations FHN-A and FHN-B by removing center nodes [55 for FHN-A and nodes (6, 41) for FHN-B]. (e) Creation of oscillations FHN-A and FHN-B by initially stimulating the centers nodes. (f) Snapshot is the same as (b) for oscillation FHN-A, with nodes placed in order. One-center target waves are displayed. (g) Snapshot is the same as (c) for oscillation FHN-B with nodes rearranged as in Fig. 2(c). Two-center target waves are observed. (h) Skeleton of oscillation FHN-A with loops passing through the pair of key nodes (55, 130) with length $L \leqslant 9$. (i) Skeleton of oscillation FHN-B. Two clusters of loops with $L \leqslant 10$ are displayed.

clusters of loops are displayed. We find that all conclusions derived from Figs. 2–6 are also applicable to Fig. 7, though the local dynamics and the coupling form are considerably different from those in Eq. (1). Moreover, the conclusions do not depend on the specific parameters given in Eqs. (1) and (2). When connective nodes are excited in sequence, principles 1 and 2 are applicable.

VII. CONCLUSIONS

In this paper we have studied pattern formation in oscillatory complex networks consisting of excitable nodes. Well-organized structures, including center nodes and skeletons, are revealed for seemingly random patterns. Two simple principles are proposed: Well-behaved target waves are demonstrated propagating from center nodes along the shortest paths; the shortest loops, which pass through both the center nodes and their drivers, dominate the network oscillations. The existence of target waves with certain centers in random networks may provide prospective insights into pattern formation in complex networks. Moreover, the discovery of skeletons will improve the understanding of crucial topological effects on the network dynamics. Based on the mechanism revealed, we are able to suppress, create, and modulate the oscillatory patterns by manipulating a few nodes. All the modulations can be predicted by analyzing the skeletons. Our surprising and useful findings are applicable to homogeneous random networks with different sizes and degrees, inhomogeneous networks, and networks with different excitable models, such as the FHN model.

In the present paper we considered periodic self-sustained oscillations in excitable complex networks. The extensions to nonperiodic and even chaotic oscillations will be our future work. The ideas and methods in the present work are expected to be applicable to wild fields where oscillatory behavior of excitable complex networks is involved, especially for neural systems. Though at present we do not consider some specific processes of neural systems, we do hope that our results may have a useful impact on the investigation of complicated neural functions, since oscillatory behavior, excitable dynamics, and complexity of interactions are crucially important for the functions of neural systems.

ACKNOWLEDGMENTS

This work was supported by the National Natural Science Foundation of China under Grant No. 10975015, the National Basic Research Program of China (973 Program) (2007CB814800), and the Science Foundation of Baoji University of Arts and Sciences under Grant No. ZK1048.

[1] D. J. Watts and S. H. Strogatz, Nature (London) **393**, 440 (1998).
[2] A.-L. Barabási and R. Albert, Science **286**, 509 (1999).
[3] A.-L. Barabási, Science **325**, 412 (2009).
[4] R. M. D'Souza, Nature Phys. **5**, 627 (2009).
[5] M. Kuperman and G. Abramson, Phys. Rev. Lett. **86**, 2909 (2001).
[6] R. Pastor-Satorras and A. Vespignani, Phys. Rev. Lett. **86**, 3200 (2001).
[7] M. Tinsley, J. Cui, F. V. Chirila, A. Taylor, S. Zhong, and K. Showalter, Phys. Rev. Lett. **95**, 038306 (2005).
[8] O. Sporns, D. R. Chialvo, M. Kaiser, and C. C. Hilgetag, Trends Cogn. Sci. **8**, 418 (2004).
[9] M. Müller-Linow, C. C. Hilgetag, and M.-T. Hütt, PLos Comput. Biol. **4**, e1000190 (2008).
[10] A. Roxin, H. Riecke, and S. A. Solla, Phys. Rev. Lett. **92**, 198101 (2004).
[11] S. Sinha, J. Saramäki, and K. Kaski, Phys. Rev. E **76**, R015101 (2007).
[12] W. Gerstner and W. M. Kistler, Spiking Neuron Models (Cambridge University Press, Cambridge, UK, 2002).
[13] E. M. Izhikevich, IEEE Trans. Neural Net. **15**, 1063 (2004).
[14] C. M. Gray, J. Comput. Neurosci. **1**, 11 (1994).
[15] G. Buzsáki and A. Draguhn, Nature(London) **304**, 1926 (2004).
[16] W. M. Usrey and R. C. Reid, Annu. Rev. Physiol. **61**, 435 (1999).
[17] M. Stopfer, S. Bhagavan, B. H. Smith, and G. Laurent, Nature (London) **390**, 70 (1997).
[18] L. M. Ward, Trends Cogn. Sci. **7**, 553 (2003).
[19] M. Steriade, D. A. McCormick, and T. J. Sejnowski, Science **262**, 679 (1993).
[20] E. Meron, Phys. Rep. **218**, 1 (1992).
[21] M. C. Cross and P. C. Hohenberg, Rev. Mod. Phys. **65**, 851 (1993).
[22] J. E. Pearson, Science **9**, 189 (1993).
[23] H. Nakao and A. S. Mikhailov, Nature Phys. **6**, 544 (2010).
[24] R. Fitzhugh, Biophys. J. **1**, 445 (1961).
[25] T. J. Lewis and J. Rinzel, Network: Comput. Neural Syst. **11**, 299 (2000).
[26] A. J. Steele, M. Tinsley, and K. Showalter, Chaos **16**, 015110 (2006).
[27] M. J. O'Donovan, Curr. Opin. Neurobiol. **9**, 94 (1999).
[28] M. V. Sanchez-Vives and D. A. McCormick, Nat. Neurosci. **3**, 1027 (2000).
[29] A. I. Selverston and M. Moulins, Annu. Rev. Physiol. **47**, 29 (1985).
[30] R. Yuste, J. N. MacLean, J. Smith, and A. Lansner, Nat. Rev. Neurosci. **6**, 477 (2005).
[31] T. P. Vogels, K. Rajan, and L. F. Abbott, Annu. Rev. Neurosci. **28**, 357 (2005).
[32] X. Liao *et al.*, Front. Phys. **6**, 124 (2011); e-print arXiv:0906.2356 (2009).
[33] Y. Qian, X. Huang, G. Hu, and X. Liao, Phys. Rev. E **81**, 036101 (2010).
[34] S. H. Strogatz, Nature (London) **410**, 268 (2001).
[35] R. Albert and A.-L. Barabási, Rev. Mod. Phys. **74**, 47 (2002).
[36] S. Boccaletti, V. Latora, Y. Moreno, M. Chavez, and D.-U. Hwang, Phys. Rep. **424**, 175 (2006).

[37] M. Bär and M. Eiswirth, Phys. Rev. E **48**, R1635 (1993).
[38] J. M. Greenberg and S. P. Hastings, SIAM J. Appl. Math. **34**, 515 (1978).
[39] P. Bak, K. Chen, and C. Tang, Phys. Lett. A **147**, 297 (1990).
[40] B. Bollobás, Modern Graph Theory (Springer-Verlag, New York, 1998).
[41] W. Jahnke and A. T. Winfree, Int. J. Bifur. Chaos **1**, 445 (1991).
[42] V. M. Eguíluz, D. R. Chialvo, G. A. Cecchi, M. Baliki, and A. V. Apkarian, Phys. Rev. Lett. **94**, 018102 (2005).